ACS APPLIED MATERIALS & INTERFACES

Research Article

www.acsami.org

Hybrid 2D Photonic Crystal-Assisted $Lu_3Al_5O_{12}$:Ce Ceramic-Plate Phosphor and Free-Standing Red Film Phosphor for White LEDs with High Color-Rendering Index

Hoo Keun Park,[†] Ji Hye Oh,[†] Heejoon Kang,[†] Jian Zhang,*[,‡] and Young Rag Do*[,†]

[†]Department of Chemistry, Kookmin University, Seoul 136-702, Republic of Korea

[‡]School of Physics and Electronic Engineering, Jiangsu Normal University, Xuzhou 221116, P. R. China

ABSTRACT: This paper reports the combined optical effects of a two-dimensional (2D) SiN_x photonic crystal layer (PCL)-assisted $Lu_3Al_5O_{12}$:Ce (LuAG:Ce) green ceramic-plate phosphor (CPP) and a free-standing (Sr,Ca)$AlSiN_3$:Eu red film phosphor to enhance luminous efficacy, color rendering index (CRI), and special CRI (R_9) of LuAG:Ce CPP-capped white light-emitting diodes (LEDs) for high-power white LEDs at 350 mA. By introducing the 2D SiN_x PCL, the luminous efficacy was improved by a factor of 1.25 and 1.15 compared to that of the conventional flat CPP-capped LED and the thickness-increased CPP-capped LED (with a thickness of 0.15 mm), respectively, while maintaining low color-rendering properties. The combining of the free-standing red film phosphor in the flat CPP-capped, the 2D PCL-assisted CPP-capped, and the thickness-increased CPP-capped LEDs led to enhancement of the CRI and the special CRI (R_9); it also led to a decrease of the correlated color temperature (CCT) due to broad wavelength coverage via the addition of red emission. High CRI (94), natural white CCT (4450 K), and acceptable luminous efficacy (71.1 lm/W) were attained from the 2D PCL-assisted LuAG:Ce CPP/free-standing red film phosphor-based LED using a red phosphor concentration of 7.5 wt %. It is expected that the combination of the 2D PCL and the free-standing red film phosphor will be a good candidate for achieving a high-power white CPP-capped LED with excellent CRI.

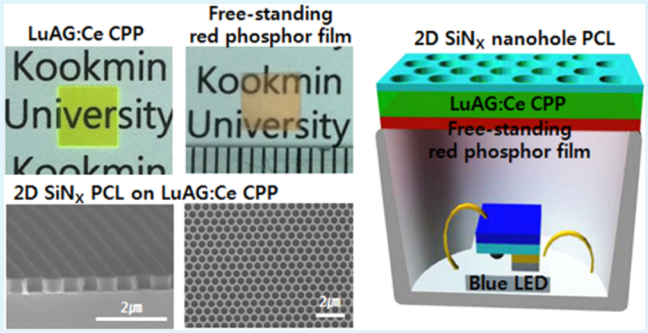

KEYWORDS: *photonic crystal, LuAG, ceramic-plate phosphor, phosphor, LED, phosphor-converted LED*

1. INTRODUCTION

Transparent ceramics have been studied and developed in the field of inorganic optical materials for application in new lasers, scintillators, and phosphors. More recently, transparent polycrystalline ceramics (TPCs), such as $Y_3Al_5O_{12}$:Ce (YAG:Ce),[1,2] $(Gd,Y)_3Al_5O_{12}$:Ce (GYAG:Ce),[3] Lu_2O_3:Eu,[4,5] and Gd_2O_2S:Pr,Ce,[6,7] have received considerable attention because their optical properties and efficiencies are comparable to or better than those of single crystals grown from the melt obtained using the Czochralski method.[8−10] In addition, these transparent polycrystalline ceramics exhibit many advantages such as high chemical homogeneity, optical transparency, doping concentration, and thermal conductivity. Because of their excellent optical and thermal properties, these TPCs are expected to be used especially for high-power solid-state lighting applications.

With the development of high-power and high-brightness solid-state lighting, interest in the use of TPCs in the field of white light-emitting diodes (LEDs) for general illumination has grown rapidly.[11−13] This is because the current leading commercial white LED (known as phosphor-converted LED, pc-LED), which consists of a combination of a blue LED chip and yellow phosphors (or green and red phosphors) packed with organic resin or silicone resin, undergoes degradation of luminous intensity, change of emission color, and deterioration of phosphor thermal quenching due to the poor thermal conductivity of the organic resin or the silicone resin. This problem becomes more and more serious with the increase of the LED chip temperature due to the increase of the output power necessary to realize high-power LEDs.[13−15] In addition, the conventional microsize powder phosphor in phosphor-in-cup typed LEDs attenuates the conversion efficiency and luminous efficacy from that of white pc-LED due to high scattering and reflecting loss of the emission from powder phosphors.[16−18] To find solutions to these issues, white LEDs incorporating a transparent polycrystalline YAG:Ce (YAG = yttrium aluminium garnet) ceramic-plate phosphor (CPP) have recently been suggested by many research groups because CPPs, compared with conventional powder phosphors in applications for white pc-LED lighting, show certain advantages such as controlled light scattering, increased longevity, and improved heat dissipation.[11,13,19−21] Quite recently, with the

Received: October 19, 2014
Accepted: February 12, 2015
Published: February 12, 2015

DOI: 10.1021/am507237n
ACS Appl. Mater. Interfaces 2015, 7, 4549−4559

aim of replacing powder phosphors with CPPs in high-power white LEDs, we reported various two-dimensional (2D) photonic crystal layer (PCL)-assisted, $Y_3Al_5O_{12}:Ce^{3+}$ (YAG:Ce) CPP-capped white LEDs exhibiting enhanced extraction efficiency and improved luminous efficacy.[22−26]

In this study, we introduce and compare the optical properties of a flat $Lu_3Al_5O_{12}$:Ce (LuAG:Ce) CPP and a 2D SiN_x PCL-assisted LuAG:Ce CPP when those materials are incorporated into white pc-LEDs. Lutetium aluminum garnet (LuAG), which is isostructural to YAG, is known to be a promising host structure.[27] LuAG doped with cerium ions (LuAG:Ce) also has been recognized as an optical material (or phosphor) and scintillator because LuAG:Ce shows larger absorption coefficient of ionizing radiation and higher quantum yield than those values of YAG:Ce.[28−31] However, the light from a LuAG:Ce phosphor-based white LED combined with a blue LED chip is colder and bluer than that from conventional incandescent and fluorescent devices, as well as even that from YAG:Ce-based white LEDs because the emission color of LuAG:Ce is green. This red deficiency of LuAG:Ce leads to a poor color rendering index (CRI) for LuAG:Ce phosphor-based white LEDs, which interrupts the realization of white LEDs with high CRI (>90) and low correlated color temperature (CCT). To solve these problems and achieve a white LED with high color rendering properties, color conversion layers with red emission in addition to green emission are essential for broad wavelength coverage.[32] For this study, to enhance the CRI and realize the white LED, we select a free-standing (Sr,Ca)$AlSiN_3$:Eu red film phosphor as a red color conversion layer and compare the effect of red phosphor, as a function of the phosphor concentration, on flat LuAG:Ce CPP-capped and 2D PCL-assisted CPP-capped white LEDs. A free-standing film type such as the CP type allows the phosphor to be less affected by the temperature of the LED chip and to be used as a pc-LED with a low binning property. Moreover, we investigate changes of the optical properties in the current/temperature dependence of 2D PCL-assisted green LuAG:Ce CPP/free-standing red bilayered type films on a blue LED cup for high-power white pc-LED applications.

2. EXPERIMENTAL METHODS

2.1. Materials. High-purity (>99.99%) Al_2O_3, Lu_2O_3, and CeO_2 powders were obtained from Shanghai Wusong Chemical Co. Ltd. as raw materials to fabricate LuAG:Ce CPP. The primary particle size of the Al_2O_3 powder was ∼250 nm, and the specific surface area of the powder was ∼11.0 g/m^2. The primary particle size of the Lu_2O_3 and CeO_2 powders was ∼60 nm, and the specific surface areas of the powders were 10.2 g/m^2 for Lu_2O_3 and ∼6.6 g/m^2 for CeO_2. Polystyrene (PS) nanospheres (with diameters of 580 nm) were purchased from Interfacial Dynamics Co. and used as a mask layer for fabricating 2D nanohole photonic crystal (PC) structures. Sodium dodecyl sulfate (SDS, $NaC_{12}H_{25}SO_4$) was obtained from Sigma-Aldrich for use in the forming of a rigid PS nanosphere monolayer. CR-7, obtained from Cyantek Co., Ltd., was used as the Cr etchant. (Sr,Ca)$AlSiN_3$:Eu red powder phosphor (R6535) was purchased from Intematix Corporation and was used to fabricate free-standing red film phosphor as a function of the phosphor concentration. OE-6636 A and B were obtained from Dow Corning Co., Ltd., and were used to create the silicone resin for encapsulation of the blue LED chips and as matrix for the fabrication of the free-standing red film phosphor. Poly(3,4-ethylenedioxythiophene):poly(styrenesulfonate) (PEDOT:PSS) was obtained from Sigma-Aldrich as sacrificial material for the fabrication of the free-standing red film phosphor.

2.2. Fabrication of Green LuAG:Ce CPP and CPP-Capped LEDs. The detailed fabrication process of the green LuAG:Ce CPP is similar to that used for fabricating the Yb:LuAG ceramics.[33,34] Briefly, the raw powders (Al_2O_3, Lu_2O_3, and CeO_2) were carefully weighed according to the LuAG:Ce chemical stoichiometric composition. The Ce doping concentration was set at 0.3 atom %. The powders were mixed with 99.99% analytical pure ethanol for ball milling. The mixed slurry was then ball milled for ∼15 h using a planetary milling machine. The milled mixtures were then dried in an oven and sieved through a 100 mesh screen. After calcining at 800 °C for 3 h to remove the organic component, the powders were dry pressed in a stainless steel die at 15 MPa to form pellets. The green body pellet was further cold isostatically pressed (CIPed) at 200 MPa. The relative green body density reached ∼53% after CIP. To achieve the theoretical density, the green body was finally sintered at 1790 °C for 12 h in a high-temperature vacuum sintering furnace under a vacuum level better than 1×10^{-4} Pa. The sample was surface polished and thermally etched at 1500 °C for 3 h to reveal the grain boundary.

To apply it to a white pc-LED as a phosphor-on-cup-type LED, the prepared thick LuAG:Ce CPP was diced using a diamond wheel, which resulted in a CPP size of 0.5 cm × 0.5 cm × thickness of 0.1, 0.15, and 0.2 mm. The diced CPP was attached to the top of a blue LED cup with silicone resin, which consists of a mixture of OE-6636 A and B at a weight ratio of 1:1.[25]

2.3. Fabrication of Triangularly Patterned 2D SiN_x Nanohole PCL on LuAG:Ce CPP-Capped LED. Triangularly patterned 2D SiN_x nanohole PC arrays were fabricated on the top surface of the prepared LuAG:Ce CPP (0.5 cm × 0.5 cm, thickness of 0.1 mm) by nanosphere lithography (NSL) and reactive ion etching (RIE) process, as described in detail elsewhere.[22,23,26,35] Briefly, SiN_x film was deposited on the LuAG:Ce CPP by plasma enhanced chemical vapor deposition (PECVD). Subsequently, a PS monolayer with a diameter of 580 nm was transferred to the SiN_x/LuAG:Ce CPP by the scooping transfer method, which led to the formation of a PS/SiN_x/CPP structure. The PS monolayer, as a deposition mask, was thinned using the O_2-based RIE process. A Cr mask layer was coated on the thinned PS/SiN_x/CPP using a thermal evaporator for selective SiN_x etching. After removing the PS nanospheres by sonication in chloroform, the Cr mask layer with nanohole arrays was clearly defined on the SiN_x/CPP structure. The Cr nanohole/SiN_x/CPP was etched using a CF_4-based RIE process to transfer the nanohole pattern to the underlying SiN_x layer. The Cr nanohole mask layer was removed using a Cr etchant (CR-7). Finally, LuAG:Ce CPP with 2D SiN_x nanohole PCL was formed.

To fabricate a white pc-LED as a phosphor-on-cup-type device, the fabricated 2D SiN_x nanohole PCL-assisted CPP was attached on top of a blue LED cup with silicone resin.

2.4. Fabrication of Free-Standing Red (Sr,Ca)$AlSiN_3$:Eu Film Phosphor and Red Phosphor-Based LED. To fabricate free-standing red film phosphor, (Sr,Ca)$AlSiN_3$:Eu red powder phosphor was mixed with silicone resin (OE-6630A, B) and then printed onto water-soluble PEDOT:PSS, which is used as a sacrificial layer, and coated on glass substrate with a 50 μm spacer. The red phosphor-printed substrate was hardened in an oven at 150 °C for 1 h. Then, the red phosphor-printed substrate was put into a water bath to delaminate the red phosphor film from the glass substrate by dissolving the PEDOT:PSS interlayer. After the PEDOT:PSS interlayer was completely removed, free-standing red film phosphor floating on the water was fabricated. Finally, the free-standing red film phosphor was picked up with tweezers and dried. To evaluate the free-standing red film phosphor according to the variation of the phosphor concentration, red powder phosphors (2.5, 5.0, 7.5, 10.0, and12.5 wt %) were mixed with silicone resin in direct proportion to the phosphor concentration. The free-standing red film phosphors fabricated with phosphor concentrations of 2.5, 5.0, 7.5, 10.0, and 12.5 wt % were attached on top of blue LED cups with silicone resin.

2.5. Fabrication of Green LuAG:Ce CPP/Free-Standing Red Film Phosphor-Based LED. To fabricate the green LuAG:Ce CPP/free-standing red film phosphor-based LED as a tricolor (RGB) pc-white LED, the free-standing red film phosphor was first attached on top of the blue LED cup. Then, the LuAG:Ce CPP and/or the 2D

DOI: 10.1021/am507237n
ACS Appl. Mater. Interfaces 2015, 7, 4549−4559

PCL-assisted CPP were attached on the red film phosphor-based LEDs.

2.6. Characterization. The optical transmittance of the fabricated LuAG:Ce CPP (thickness of 0.1 mm) was measured over the wavelength region from 300 to 800 nm using a UV−vis spectrophotometer (OPTIZEN 2120UV, MECASYS). The LuAG:Ce CPP and free-standing (Sr,Ca)$AlSiN_3$:Eu red film phosphor was photographed using an NEX-5 (SONY) camera. The crystal structure of the LuAG:Ce CPP was measured by X-ray diffraction (XRD, X'pert system, Philips) with Cu Kα_1 radiation. The diffraction patterns were obtained over a range of 10−80° 2θ at a scan rate of 1° 2θ/min. Cross-sectional and surface images of the LuAG:Ce CPP and 2D SiN_x nanohole-assisted LuAG:Ce CPP were obtained by field-emission scanning electron microscopy (FESEM) (JSM 7401F, JEOL) operated at 10 kV. Using a spectrophotometer (PSI Co. Ltd. model Darsapro-5000), the photoluminescence (PL) and excitation (PLE) spectra from the LuAG:Ce CPP and from the (Sr,Ca)$AlSiN_3$:Eu red powder phosphor were measured under the excitation wavelength at 450 nm and the emission wavelength at 515 nm (450 and 640 nm in the case of red phosphor) by Xe-lamp, respectively. The electroluminescent (EL) properties (such as electroluminescence spectra, luminous efficacy, CIE color coordinates, correlated color temperature, color rendering index, and special color rendering index) of the LuAG:Ce CPP, 2D PCL-assisted LuAG:Ce CPP, free-standing red film phosphor, and 2D PCL-assisted CPP/free-standing red film phosphor capped on top of blue InGaN LED cup were measured using a spectrophotometer (PSI Co. Ltd. Model Darsa II) with integrating spheres under equal current. These properties were also measured for the 2D PCL-assisted CPP/free-standing red film phosphor as functions of the applied current and the ambient temperature.

3. RESULTS AND DISCUSSION

Figure 1 provides schematic diagrams of four different white LED structures: the conventional flat LuAG:Ce CPP-capped white LED [c-flat CPP](Figure 1a); the 2D SiN_x PCL-assisted CPP-capped LED [SiN_x-PCL CPP] (Figure 1b); the flat LuAG:Ce CPP/free-standing red film phosphor-based LED [c-flat CPP/f-film] (Figure 1c); and the 2D PCL-assisted CPP/free-standing red film phosphor-based LED [SiN_x-PCL CPP/f-film] (Figure 1d). All white LEDs are phosphor-on-cup type LEDs, and yet are different from the phosphor-in-cup type of the conventional powder-based white LED. The fabrication procedures for all white LEDs are described in detail in the Experimental Section.

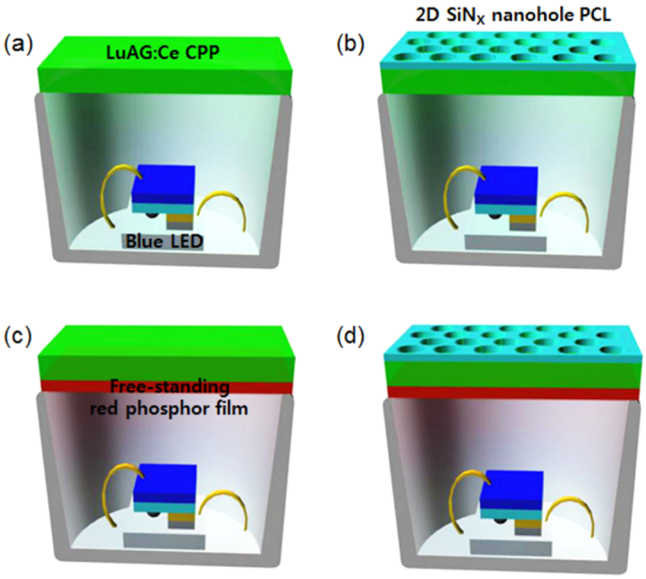

Figure 1. Schematic diagrams of four different white LED structures: (a) conventional flat LuAG:Ce CPP-capped white LED [c-flat CPP], (b) 2D SiN_x PCL-assisted CPP-capped LED [SiN_x-PCL CPP], (c) flat LuAG:Ce CPP/free-standing red film phosphor-based LED [c-flat CPP/f-film], and (d) 2D PCL-assisted CPP/free-standing red film phosphor-based LED [SiN_x-PCL CPP/f-film].

Figure 2 shows the optical, structural, and morphological properties of the LuAG:Ce CPP (0.1 mm thickness). The optical transmittance of LuAG:Ce CPP is ∼80% above 500 nm, as shown in Figure 2a, indicating that the CPP is optically transparent in the range of visible light. The absorption bands at ∼345 and 450 nm are related to 5d and 4f transitions of Ce^{3+} ions, respectively.[30,36] The inset of Figure 2a shows a photograph of LuAG:Ce CPP (0.5 cm × 0.5 cm × thickness of 0.1 mm) exhibiting high transparency. The letters can be read clearly through the CPP. The XRD patterns shown in Figure 2b indicate that the phase of the LuAG:Ce CPP corresponds to that of previously reported LuAG:Ce ceramics;[30,31] no other phases were detected, demonstrating the good solubility of Ce^{3+} in the LuAG host lattice. The observed patterns are found to match well with the standard card of JCPDS 73−1368. Top and side view SEM images of the LuAG:Ce CPP shown in Figure 2c indicate that the CPP has a smooth and planar surface of thick film-type phosphor form. In addition, Figure 2d displays the excitation (λ_{em} = 515 nm) and emission (λ_{ex} = 450 nm) spectra of the LuAG:Ce CPP. These spectra confirm that the LuAG:Ce CPP exhibits a broadband emission covering a range from 470 to 650 nm under 450 nm excitation, and it indicates that the CPP can be used as a film-type phosphor for application in white pc-LEDs using blue LEDs.

Because the film-type LuAG:Ce CPP has a low extraction efficiency as a result of its total internal reflection (TIR) and waveguide effect, a 2D PCL that produces leaky and/or Bragg scattering is necessary to improve the extraction efficiency of CPP with high brightness. Figure 3a provides schematic diagrams of the fabrication process of the triangularly patterned 2D SiN_x nanohole PC structure on the LuAG:Ce CPP. The top and side view SEM images of the 2D SiN_x PCL-assisted LuAG:Ce CPP shown in Figure 3b indicate that the 2D SiN_x nanohole array was successfully fabricated on the LuAG:Ce CPP by the NSL and RIE processes. The fabricated 2D SiN_x PCL-assisted LuAG:Ce CPP was attached on top of a blue LED cup for implementation of the white pc-LED. Figure 3c shows the EL emission spectra of the conventional flat LuAG:Ce CPP-capped LED (called a c-flat CPP), the 2D SiN_x PCL-assisted CPP-capped LED (called a SiN_x-PCL CPP), and the thickness-increased flat CPP-capped LED (with thickness of 0.15 and 0.2 mm, correspondingly referred to as the thick-flat CPP-0.15 and the thick-flat CPP-0.2) at equal current (350 mA). The intensity of the green emission and the luminance of the SiN_x-PCL CPP were higher than those of the c-flat CPP due to the introduction of a 2D SiN_x nanohole PCL on top of the CPP. The 2D PCL can lead to a reduction of the blue LED light transmitted through the 2D PCL-coated CPP by backscattering of the excitation and enhancement of the green emission via reabsorption through backscattering and a leaky mode of emission.[22−26] The intensity of the green emission and the luminance of the thick-flat CPP-0.15 and the thick-flat CPP-0.2 were also higher than those of the c-flat CPP due to the increase in the thickness of the CPP. However, increasing the thickness of the CPP to improve the intensity of the green emission led to a similar external quantum yield of

DOI: 10.1021/am507237n
ACS Appl. Mater. Interfaces 2015, 7, 4549−4559

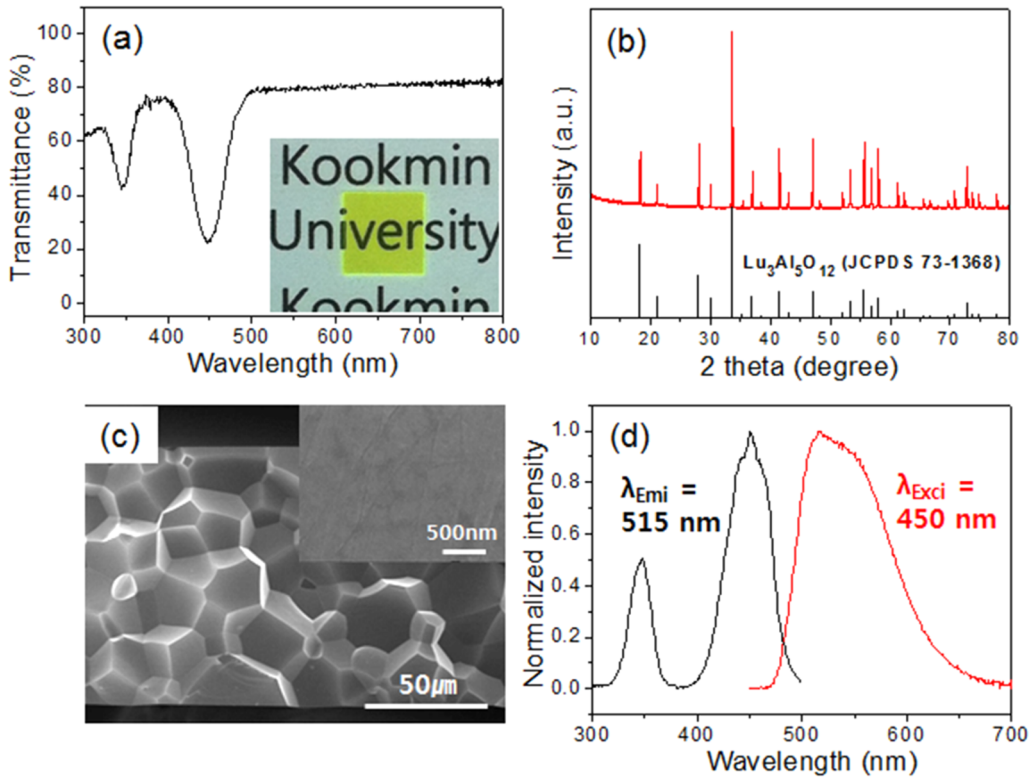

Figure 2. (a) Optical transmittance, (b) XRD patterns, (c) top and side view SEM images, and (d) excitation (λ_{em} = 515 nm) and emission (λ_{ex} = 450 nm) spectra of a conventional flat LuAG:Ce CPP (0.1 mm thickness). The inset in (a) provides a photograph of the LuAG:Ce CPP (0.5 cm × 0.5 cm × thickness of 0.1 mm), showing that it is highly transparent.

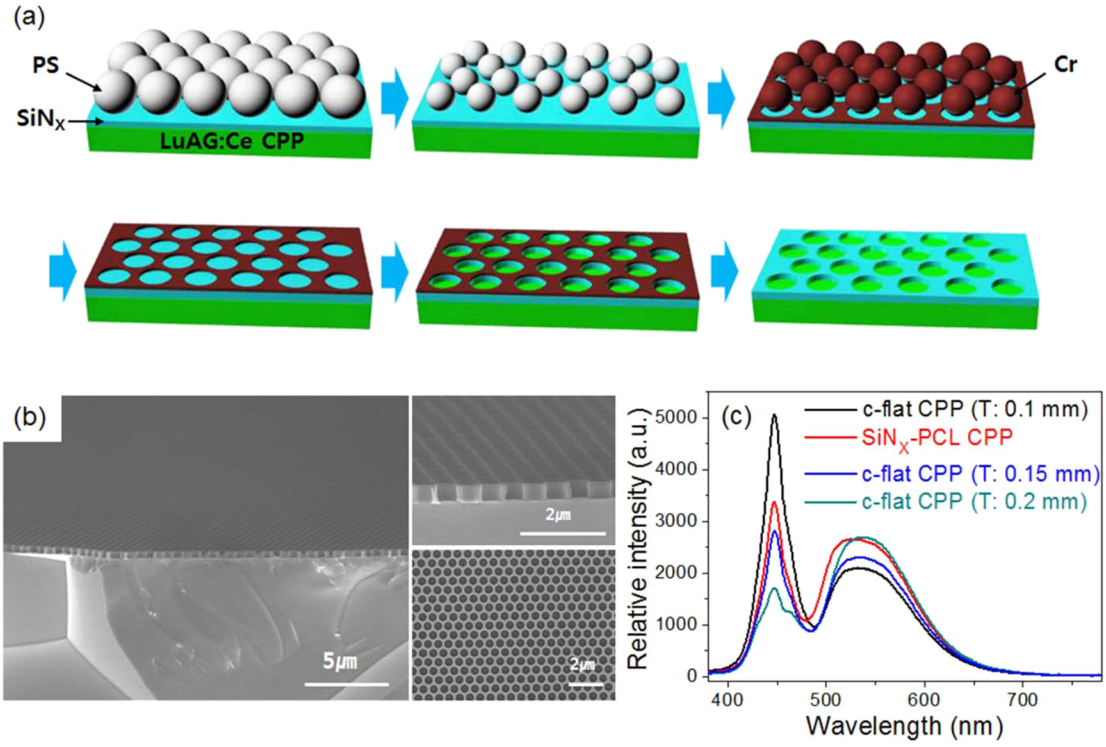

Figure 3. (a) Schematic diagrams of the fabrication process and (b) top and side view SEM images of the triangularly patterned 2D SiN_x nanohole PC structure on the flat LuAG:Ce CPP. (c) Electroluminescent (EL) emission spectra of the conventional flat LuAG:Ce CPP-capped LED, the 2D SiN_x PCL-assisted CPP-capped LED, and the thickness-increased flat CPP-capped LED (with thicknesses of 0.15 and 0.2 mm) at equal-current (350 mA).

DOI: 10.1021/am507237n
ACS Appl. Mater. Interfaces 2015, 7, 4549−4559

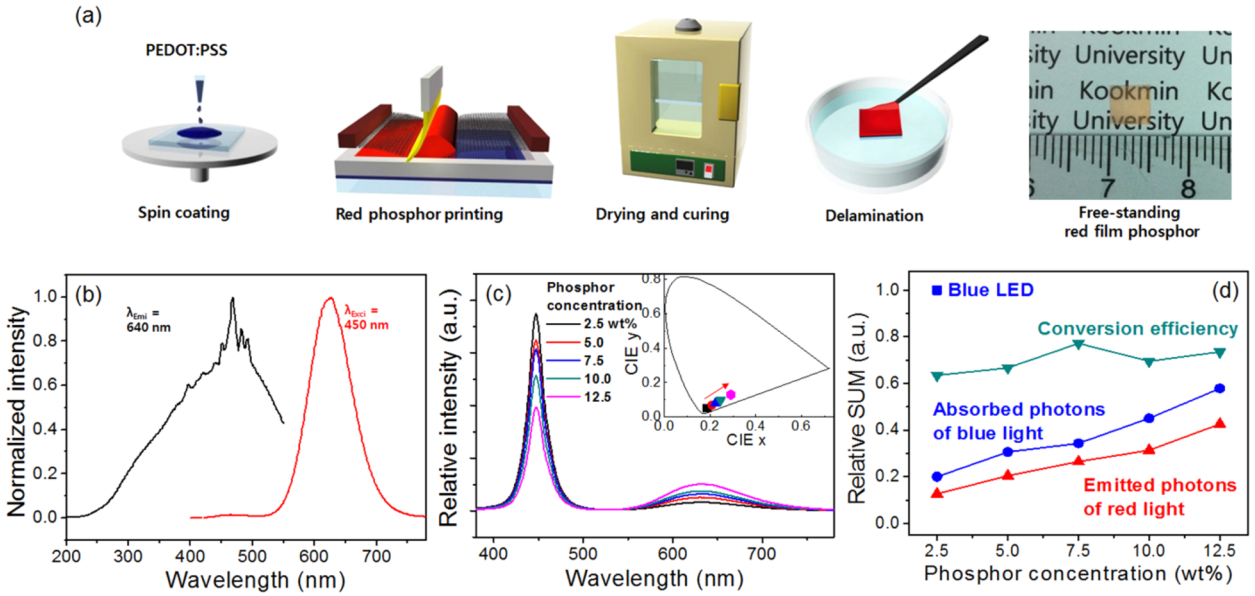

Figure 4. (a) Schematic diagrams of the fabrication process and (b) excitation (λ_{em} = 640 nm) and emission (λ_{ex} = 450 nm) spectra of the (Sr,Ca)$AlSiN_3$:Eu red powder phosphor. (c) Electroluminescent (EL) emission spectra, CIE color coordinates, and (d) the relative sum of absorbed photons of the blue light, the relative sum of emitted photons of the red light, and the conversion efficiency of the free-standing red film phosphor on top of blue LED cup as functions of the phosphor concentration (2.5, 5.0, 7.5, 10.0, and 12.5 wt %). The relative sum was compared with the sum of the emitted photons of a blue LED.

the CPP on the basis of the conversion efficiency (CE) as calculated from the measured EL emission spectra. The CE is the ratio of the extracted light of the phosphor layer from the pc-LED packaging to the blue light spent in the pc-LED package to be converted to phosphor light, or, in other words, the ratio between the number of emitted photons and number of incident photons.[23] The CEs of the c-flat CPP, SiN_x-PCL CPP, thick-flat CPP-0.15, and thick-flat CPP-0.2 were ~0.64, 0.70, 0.62, and 0.63, respectively. This indicates that the fabrication of the SiN_x-PCL CPP leads to an improvement of the external quantum yield of the LuAG:Ce CPP owing to the enhanced extraction efficiency, while the thick-flat CPPs (0.15 and 0.2 mm) show similar external quantum yields of the CPP. This also indicates that, by increasing the thickness of the CPP, the intensity of the green emission of the CPP can be increased, whereas the blue emission is significantly decreased compared to the decrease of the blue emission from the introduction of the 2D PCL. These results also confirm that the fabrication of the SiN_x-PCL CPP is much more suitable for improving the intensity of the green emission and the external quantum yield of the CPP compared to the thickness-increased CPP with a similar spectral power distribution (SPD). The luminous efficacy of the SiN_x-PCL CPP was 94.3 lm/W, which is ~1.25, 1.15, and 1.01 times higher than those of the c-flat CPP (75.7 lm/W), the thick-flat CPP-0.15 (81.8 lm/W), and the thick-flat CPP-0.2 (93.4 lm/W), respectively, at the same applied current. The CCT (~8140 K) of the SiN_x-PCL CPP changed to a low value compared with that (~16670 K) of the c-flat CPP after the introduction of the 2D PCL on the CPP, which indicates that the CPP-based LED changes to desirable white colors with the assistance of the 2D PCL. The CCTs (7770 and 6450 K) of the thick-flat CCP-0.15 and thick-flat CPP-0.2 also changed to a low value compared to that of the c-flat CPP after increasing the thickness of the CPP. However, the green emission color from LuAG:Ce CPP not only makes the fabrication of white LED with low CCT (~4500 K) difficult but also inhibits the realization of white LED with high CRI (>90) when the CPP is implemented in a white pc-LED package. For these reasons, although the 2D PCL was fabricated on the CPP, the variation of the CCT was very limited. Moreover, the CRIs and the R_9 values of the c-flat CPP, the SiN_x-PCL CPP, the thick-flat CPP-0.15, and the thick-flat CPP-0.2 were low regardless of the introduction of the 2D PCL and the increase in the thickness of the CPP. The R_9 is a special CRI that imparts a strong red value with the aim of achieving a high-quality color rendition of the light source.[37] A high CRI cannot guarantee good saturated colors of illuminated objects because CRI is calculated with only the first eight values (R_1–R_8) of CIE from the recommended 14 test color samples that are normally used for the calculation of the CRI.[38,39] Therefore, to address this problem, an evaluation standard using a strong red value (special CRI, R_9) is needed.

To recover the red deficiency of the LuAG:Ce CCP and achieve a white pc-LED that is implemented with a CPP exhibiting low CCT, high CRI, and high R_9, the free-standing (Sr,Ca)$AlSiN_3$:Eu red film phosphor was introduced in the LuAG:Ce CPP-based white LED package. Figure 4 provides schematic diagrams of the fabrication process of the free-standing (Sr,Ca)$AlSiN_3$:Eu red film phosphor. To evaluate the optical properties of the (Sr,Ca)$AlSiN_3$:Eu red powder phosphor, its excitation (λ_{em} = 640 nm) and emission (λ_{ex} = 450 nm) spectra were measured, with results shown in Figure 4b. The excitation spectrum exhibited a broad absorption band from the near-UV to the yellow region (300–550 nm). The emission spectrum displayed a single broad band centered at 640 nm; this band was attributed to the $4f^65d^1$–$4f^7$ transition of Eu^{2+}.[40] Figure 4c,d shows the EL emission spectra, CIE color coordinates, the relative sum of the absorbed photons of the blue light, the relative sum of emitted photons of the red light, and the conversion efficiency (i.e., the ratio of emitted photons to absorbed photons) of the free-standing red film phosphors as a function of the phosphor concentration (2.5, 5.0, 7.5, 10.0,

DOI: 10.1021/am507237n
ACS Appl. Mater. Interfaces 2015, 7, 4549–4559

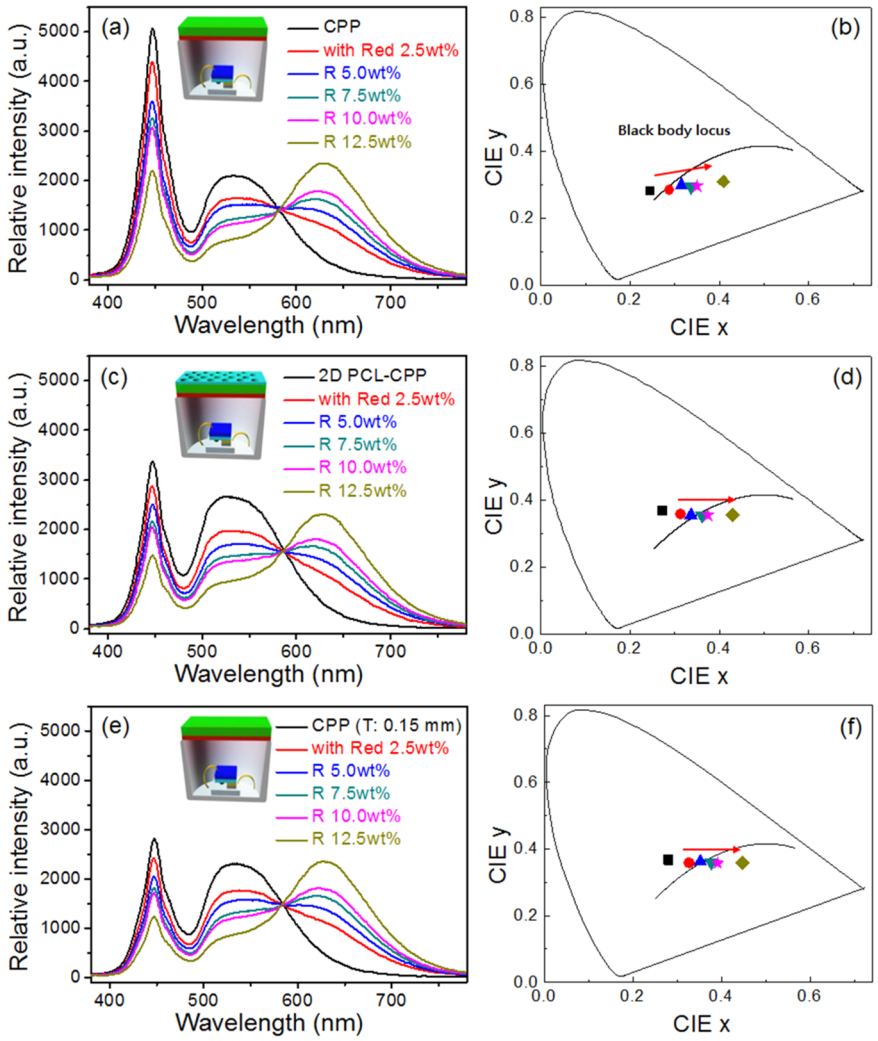

Figure 5. (a, c, and e) Electroluminescent (EL) emission spectra, and (b, d, and f) CIE color coordinates of the LuAG:Ce CPP/free-standing red film phosphor-based LED, the 2D PCL-assisted CPP/free-standing red film phosphor-based LED, and the thickness-increased CPP (0.15 mm)/free-standing red film phosphor-based LED as functions of the red phosphor concentration at equal current (350 mA).

and 12.5 wt %) in silicone resin when the phosphors are incorporated into pc-LEDs. The relative sum was compared with the sum of the emitted photons of a blue LED. As the phosphor concentration increased, the intensity of the red emission and the luminance of the free-standing red phosphor-capped LEDs increased due to the enhanced absorption of red phosphor from the blue LED light, as shown in Figure 4c. The CIE color coordinates of the free-standing film phosphors shifted from blue to reddish due to the increased ratio of red to blue in the emission spectrum with the increase of the phosphor concentration, as shown in the inset of Figure 4c. Likewise, Figure 4d shows that the absorbed photons of the blue light and the emitted photons of the red light of the free-standing film phosphors increased as the phosphor concentration increased. The CEs of the free-standing film phosphors reached ~0.63−0.77. These results indicate that the free-standing film phosphors can be used as red phosphors in green/red-based pc-LEDs to realize low CCT, high CRI, and high R_9; these film phosphors can also be applied to various pc-LED packages.

Figure 5a−f compares the EL emission spectra and CIE color coordinates of the flat LuAG:Ce CPP/free-standing red film phosphor-based LED (called a c-flat CPP/f-film), the 2D PCL-assisted CPP/free-standing red film phosphor-based LED (called an SiN_x-PCL CPP/f-film), and the thickness-increased CPP (with a thickness of 0.15 mm)/free-standing red film phosphor-based LEDs (called the thick-flat CPP-0.15/f-film) as functions of the red phosphor concentration at equal current (350 mA). The thick-flat CPP-0.15/f-film was selected because the SPD of the thick-flat CPP-0.15 is similar to that of the SiN_x-PCL CPP/f-film. To fabricate a tricolor (RGB) white LED, a free-standing red film phosphor was first attached on top of a blue LED cup, and then a flat LuAG:Ce CPP, the 2D PCL-assisted CPP, and thickness-increased CPPs (0.15 mm) were attached on the red film phosphor-based LED. The green emission portion of the white color decreased, but the red portion of the white color increased with the increase of red phosphor concentration regardless of the introduction of the 2D PCL on the LuAG:Ce CPP and the increase in thickness of the CPP, as shown in Figure 5a,c,e. As the red phosphor concentration increased, the CIE color coordinates of the c-flat CPP/f-film, the SiN_x-PCL CPP/f-film, and the thick-flat CPP-0.15/f-film shifted from bluish or greenish-white to reddish-white due to the increased ratio of red to blue/green in the emission spectrum, as shown in Figure 5b,d,f. The thick-flat CPP-0.15/f-film exhibited similar EL emission spectra and CIE

DOI: 10.1021/am507237n
ACS Appl. Mater. Interfaces 2015, 7, 4549−4559

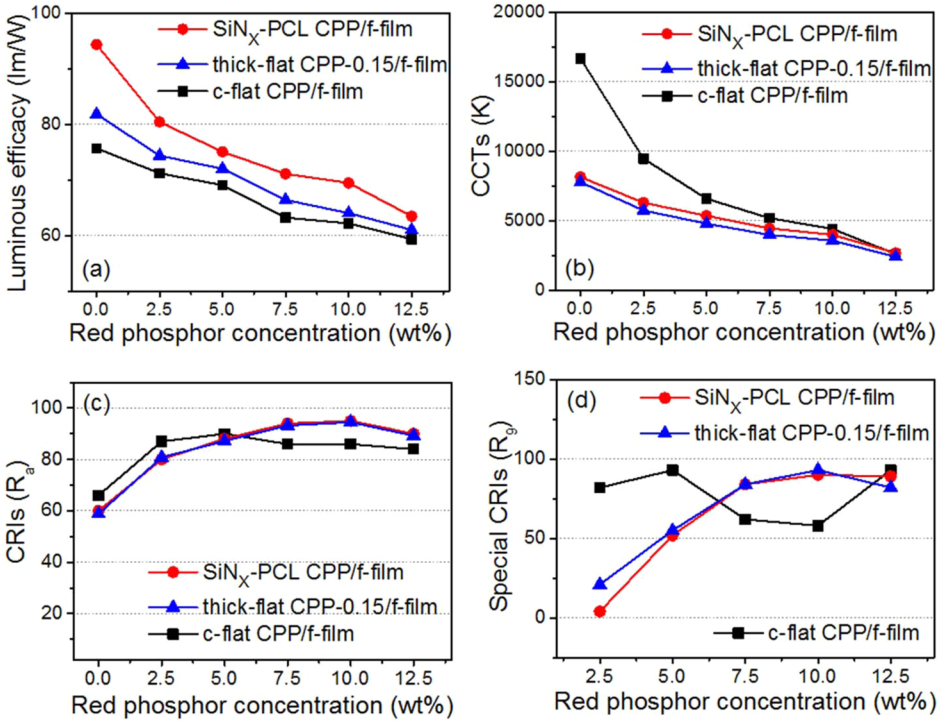

Figure 6. (a) Luminous efficacy (lm/W), (b) CCTs, (c) CRIs, and (d) special CRIs of the LuAG:Ce CPP/free-standing red film phosphor-based LED, the 2D PCL-assisted CPP/free-standing red film phosphor-based LED, and the thickness-increased CPP (0.15 mm)/free-standing red film phosphor-based LED as functions of the red phosphor concentration at equal current (350 mA).

color coordinates compared with the SiN_x-PCL CPP/f-film because they have similar SPDs. In addition, the color coordinates of the SiN_x-PCL CPP/f-film and thick-flat CPP-0.15 were significantly closer to the blackbody locus than those of the c-flat CPP/f-film as a function of the red phosphor concentration. This indicates that the SiN_x-PCL CPP/f-film with a small D_{uv} (D_{uv} indicates the distance from the blackbody locus on the CIE 1960 chromaticity diagram) as a result of the 2D PCL and the thick-flat CPP-0.15 with a small D_{uv} as a result of the increase of the thickness were more suitable candidates for application in high-power white LEDs than the c-flat CPP/f-film with a large D_{uv}. These results also indicate that, through varying the red phosphor concentration, an optimized white pc-LED with low CCT, high CRI, and high R_9 can be fabricated because the white color is made with a balance of blue, green, and red light. Figure 6 shows the luminous efficacy (lm/W), CCTs, CRIs, and R_9 of the c-flat CPP/f-film, SiN_x-PCL CPP/f-film, and thick-flat CPP-0.15/f-film as functions of the red phosphor concentration at equal current (350 mA). The luminous efficacies of the c-flat CPP/f-films, SiN_x-PCL CPP/f-films, and thick-flat CPP-0.15/f-films decreased as the red phosphor concentration increased, while the luminous efficacies of the SiN_x-PCL CPP/f-films were greater than those of the c-flat CPP/f-films and thick-flat CPP-0.15/f-films under all red phosphor concentrations due to the effect of the 2D PCL, as shown in Figure 6a. This is because the green emission portion of the white color decreased, but the red portion of the white color increased with the increase of the red phosphor concentration. The luminous efficacy of radiation (or LER), in lumens per watt (lm/W), is a parameter describing how bright the radiation is perceived to be by the average human eye.[37,41] As the eye sensitivity peaks at 555 nm, the highest possible LER (683 lm/W) is obtained from monochromatic green radiation at 555 nm. Therefore, any other spectrum will yield a lower LER because the human eye is less sensitive to other wavelengths. For this reason, to realize white light, there is no choice but to set the LER of white light significantly lower than 683 lm/W because red and blue emission should be used. The SiN_x-PCL CPP/f-films have higher luminous efficacies compared to the thick-flat CPP-0.15/f-films because the EL intensity of the SiN_x-PCL CPP is higher than that of the thick-flat CPP-0.15, although the SPD of the SiN_x-PCL CPP is similar to that of the thick-flat CPP-0.15. The CCTs of the c-flat CPP/f-films, the SiN_x-PCL CPP/f-films, and the thick-flat CPP-0.15/f-films decreased from 16 670 to 2600 K, from 8140 to 2680 K, and from 7770 to 2400 K with the increase of the red phosphor concentration from 0.0 to 12.5 wt % (Figure 6b). Under all red phosphor concentrations, the CCTs of the SiN_x-PCL CPP/f-films and the thick-flat CPP-0.15/f-films were lower than those of the c-flat CPP/f-films. This difference is attributed to the increase in green emission from the CPP and the decrease of transmitted blue light from the blue LED chip, due to leaky and/or Bragg scattering by the 2D PCL and to the increase in the thickness of the CPP. The CRIs of the c-flat CPP/f-films and the CRIs of the SiN_x-PCL CPP/f-films and thick-flat CPP-0.15/f-films, shown in Figure 6c, crossed over at a red phosphor concentration of 7.5 wt %. At a concentration more than 7.5 wt %, the SiN_x-PCL CPP/f-films and thick-flat CPP-0.15/f-films exhibited CRIs of more than 90, while the c-flat CPP/f-films showed CRIs below 90. In addition, the R_9 values of the c-flat CPP/f-films, the SiN_x-PCL CPP/f-films, and the thick-flat CPP-0.15/f-films increased significantly due to the addition of free-standing red phosphor films. As the SPD of the SiN_x-PCL CPP is similar to that of the thick-flat CPP-0.15, the CRIs and R_9 values of the SiN_x-PCL CPP/f-films and thick-flat CPP-0.15/f-films were similar. These results clearly confirm that white LED with high CRI and R_9 was fabricated successfully using the 2D PCL-assisted LuAG:Ce CPP and

DOI: 10.1021/am507237n
ACS Appl. Mater. Interfaces 2015, 7, 4549−4559

free-standing red film phosphor on top of blue LED of phosphor-on-cup-type. It is also possible to fabricate a white LED with high CRI and R_9 values with the thickness-increased CPP and free-standing red film phosphor. However, the SiN_x-PCL CPP is more suitable for improving the intensity of the green emission and the external quantum yield of the CPP compared to the thick-flat CPP-0.15 on the basis of the CEs calculated from the measured EL emission and the luminous efficacy. Therefore, these results demonstrate that, instead of using only conventional CPPs, a combination of 2D PCL-assisted LuAG:Ce CPP and free-standing red film phosphor can be applied to achieve a more efficient white pc-LED package exhibiting low CCT, high CRI (>90), and high R_9.

To further evaluate the suitability of the SiN_x-PCL CPP/f-film for use in high-power white LEDs, the detailed EL properties were measured as functions of the applied current and the environmental temperature. As the best optimized sample among the various SiN_x-PCL CPP/f-films with six different red phosphor concentrations, we selected the SiN_x-PCL CPP/f-film with the red phosphor concentration of 7.5 wt % because it not only realized a natural white CCT (4450 K), as specified by the American National Standards Institute (ANSI) standard (C78.377−2008), but also exhibited an excellent CRI (94) and acceptable luminous efficacy (71.1 lm/W). We compared the c-flat CPP/f-film with a red phosphor concentration of 10.0 wt % (4410 K), which has a similar CCT, with the SiN_x-PCL CPP/f-film with a red phosphor concentration of 7.5 wt % (4450 K). We also compared the thick-flat CPP-0.15/f-film with a red phosphor concentration of 7.5 wt %, which has a similar SPD, with the SiN_x-PCL CPP/f-film with a red phosphor concentration of 7.5 wt %. Figure 7 shows the EL emission spectra of the c-flat CPP/f-film with a red phosphor concentration of 10.0 wt %, the SiN_x-PCL CPP/f-film with a red phosphor concentration of 7.5 wt %, and the thick-flat CPP-0.15/f-film with a red phosphor concentration of 7.5 wt %. The EL emission spectrum of the SiN_x-PCL CPP/f-film with a red phosphor concentration of 7.5 wt % is fairly similar to that of the thick-flat CPP-0.15/f-film with a red phosphor concentration of 7.5 wt %. Although the EL emission spectra (or SPDs) of the c-flat CPP/f-film and the SiN_x-PCL CPP/f-film are different, to show the effect of the 2D SiN_x PCL on flat CPP, the comparison between the c-flat CPP/f-film with a red phosphor concentration of 10.0 wt % (4410 K) and the SiN_x-PCL CPP/f-film with a red phosphor concentration of 7.5 wt % (4450 K) is necessary when their CCTs are similar. For this reason, we compare plots of the luminous flux (lm), luminous efficacy, CRI, and CIE color coordinates for the c-flat CPP/f-film with red phosphor concentrations of 10.0 wt %, the SiN_x-PCL CPP/f-film with red phosphor concentrations of 7.5 wt %, and the thick-flat CPP-0.15/f-film with red phosphor concentration of 7.5 wt %, respectively, as functions of the applied current and the environment temperature (Figure 8). The SiN_x-PCL CPP/f-film exhibited a relatively high luminous flux, luminous efficacy, and CRI and a similar variation of color coordinates compared with the c-flat CPP/f-film with an increase in the applied current and environment temperature. The thick-flat CPP-0.15/f-film showed a relatively low luminous flux and luminous efficacy and similar variations of the CRI and color coordinates compared with the SiN_x-PCL CPP/f-film with an increase in the applied current and environment temperature. These outcomes arose because the EL intensity of the thick-flat CPP-0.15/f-film is lower than that of the SiN_x-PCL CPP/f-film (see Figure 7), although the SPD of the thick-flat CPP-0.15 is similar to that of the SiN_x-PCL CPP. The luminous efficacy of the c-flat CPP/f-film, the SiN_x-PCL CPP/f-film, and the thick-flat CPP-0.15/f-film decreased from 81.5 to 45.8 lm/W, from 93.6 to 50.6 lm/W, and from 87.2 to 48.0 lm/W, respectively, with an increase in the applied current from 50 to 700 mA as shown in Figure 8a. It also indicates that the luminous efficacy of the SiN_x PCL CPP/f-film was improved by factors of 1.14 and 1.07 at 350 mA compared with that of the conventional flat c-flat CPP/f-film at similar CCTs and compared to the thick-flat CPP-0.15/f-film at similar SPDs, respectively. With the introduction of 2D PCL and the increase of the CPP thickness, CRI, and CIE color coordinates of the c-flat CPP/f-film and SiN_x-PCL CPP/f-film remained almost constant or changed only slightly regardless of the applied current (see Figure 8b,c). In addition, Figure 8d−f shows that variations of the luminous flux, luminous efficacy, CRI, and CIE color coordinates for the c-flat CPP/f-film, the SiN_x-PCL CPP/f-film, and the thick-flat CPP-0.15/f-film are very small or almost constant regardless of the ambient temperature. Thus, the SiN_x-PCL CPP/f-film and thick-flat CPP-0.15/f-film are more suitable for application to high-power white LEDs than the c-flat CPP/f-film. However, the thick-flat CPP-0.15/film exhibited lower external quantum yield and the luminous efficacy values compared with the SiN_x-PCL CPP/f-film. These results confirm that the SiN_x-PCL CPP/f-film has good current and thermal stability, making it applicable for use in high-power white LEDs.

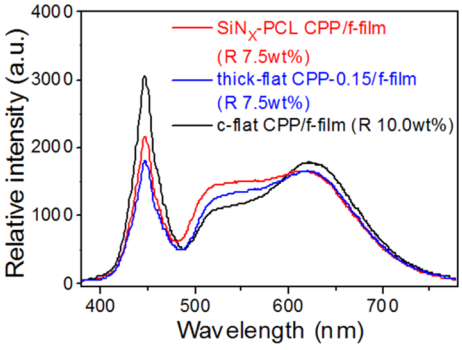

Figure 7. EL emission spectra of the flat LuAG:Ce CPP/free-standing red film phosphor-based LED, the 2D PCL-assisted CPP/free-standing red film phosphor-based LED, and the thickness-increased CPP/free-standing red film phosphor-based LED with red phosphor concentrations of 10.0, 7.5, and 7.5 wt %, respectively.

Figure 9 plots the measured relative lumens and color coordinates as a function of the viewing angle for the c-flat CPP/f-film (red phosphor concentration: 10.0 wt %) and SiN_x-PCL CPP/f-film (7.5 wt %) obtained under identical excitation conditions (current: 350 mA). The c-flat CPP/f-film exhibited a stronger edge-emission pattern compared with the SiN_x-PCL CPP/f-film. This resulted from the strong waveguide effect at the interface between the surface of the flat CPP and the air. This effect can be resolved through introducing the 2D PCL, which helps focus more emitted light toward the viewers of white lighting devices. The normally directed emission of the SiN_x-PCL CPP/f-film was significantly higher than that of the c-flat CPP/f-film. In addition, the angular dependence of the color coordinates from the SiN_x-PCL CPP/f-film was more stable than that of the c-flat CPP/f-film, as seen in Figure 9b. These results indicate that the SiN_x-PCL CPP/f-film exhibited a significantly improved normally directed EL emission and a

DOI: 10.1021/am507237n
ACS Appl. Mater. Interfaces 2015, 7, 4549−4559

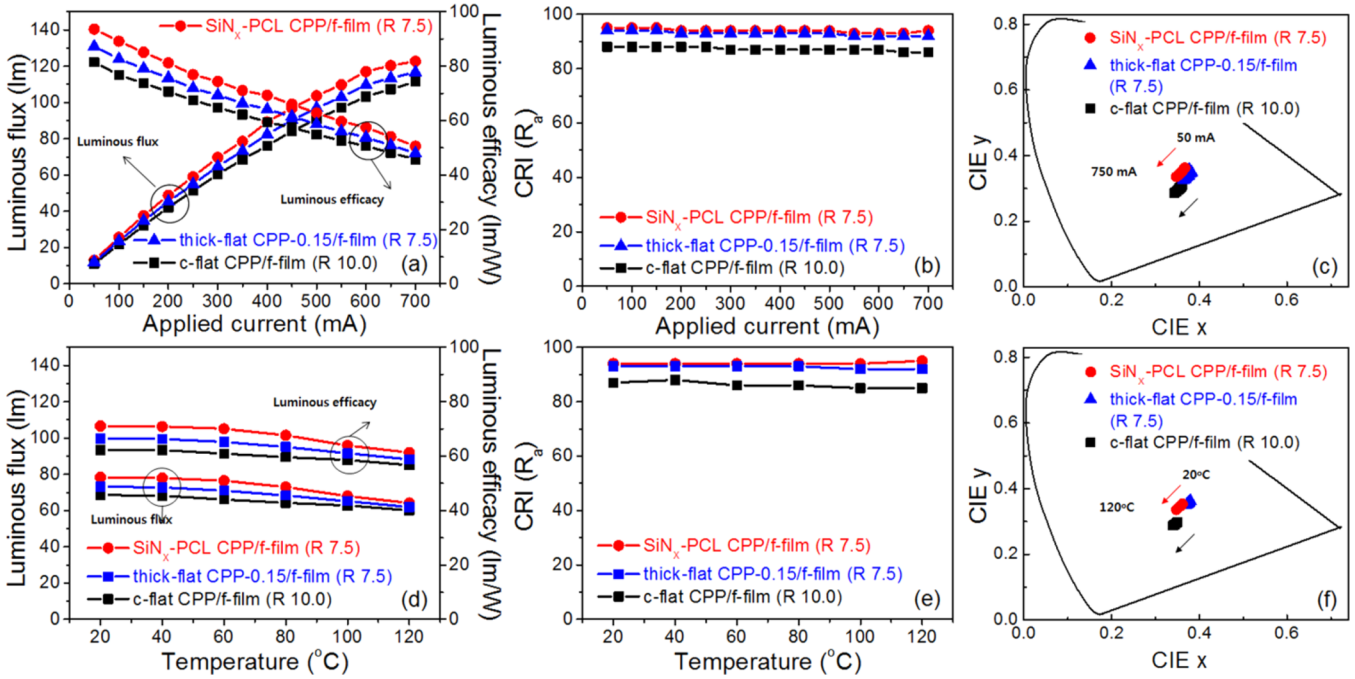

Figure 8. (a, d) Luminous flux (lm), luminous efficacy, (b, e) CRI, and (c, f) CIE color coordinates for the flat LuAG:Ce CPP/free-standing red film phosphor-based LED, the 2D PCL-assisted CPP/free-standing red film phosphor-based LED, and the thickness-increased CPP/free-standing red film phosphor-based LED with red phosphor concentrations of 10.0, 7.5, and 7.5 wt %, respectively, as functions of the applied current and the environment temperature.

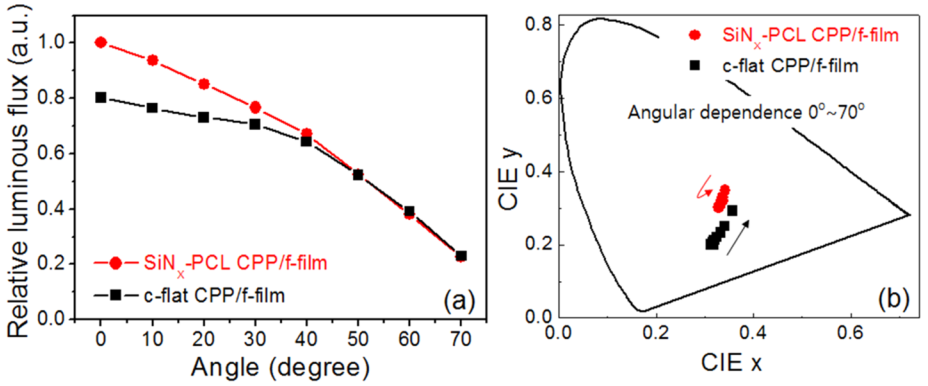

Figure 9. (a) Measured relative lumens and (b) color coordinates as a function of the viewing angle for the c-flat CPP/f-film (red phosphor concentration: 10.0 wt %) and SiN_x-PCL CPP/f-film (7.5 wt %) under identical excitation conditions (current: 350 mA).

lower color shift compared with the c-flat CPP/f-film. Therefore, these results clearly indicate that the SiN_x-PCL CPP/f-film provides acceptable luminous efficacy, low CCT, excellent CRI, high current, acceptable thermal stability, and stable angular dependence on the emission.

4. CONCLUSION

A 2D SiN_x nanohole PCL and free-standing (Sr,Ca)$AlSiN_3$:Eu red film phosphor were proposed and demonstrated to enhance luminous efficacy and CRI of LuAG:Ce CPP-capped white LEDs with the aim of achieving high-power and stable white LEDs exhibiting excellent CRI. The luminous efficacy (94.3 lm/W) of the 2D PCL-assisted LuAG:Ce CPP-capped LED was 25 and 15% higher than that of a flat CPP-capped LED (75.7 lm/W) and a thickness-increased CPP-capped LED (with a thickness of 0.15 mm) (81.8 lm/W), respectively. Moreover, the addition of 2D PCL and the increase of the CPP thickness changed high CCT (~16670 k) of the flat CPP-capped LED to somewhat lower CCTs (~8140 and 7770 K), respectively, due to the combined effect of the increase of the green emission from the CPP and the decrease of the transmitted blue light from the blue LED chip owing to leaky and/or Bragg scattering by the 2D PCL and to the increase in the thickness of the CPP. The EL emission and the luminous efficacy results indicate that the 2D PCL-assisted CPP-capped LED is more suitable for improving the intensity of the green emission and the external quantum yield of the CPP compared to the thickness-increased CPP-capped LED. When a free-standing red film phosphor was introduced between the 2D PCL-assisted or flat LuAG:Ce CPPs and the blue LED cup, our package, as a function of the red phosphor concentration, exhibited higher CRI and special CRI (R_9) and lower CCT than those values of the 2D PCL-assisted CPP-capped LED. Among the various red phosphor concentrations (0.0, 2.5, 5.0, 7.5, 10.0, 12.5 wt %) in this experiment, the LED package with red phosphor concentration of 7.5 wt % showed an excellent CRI (94), high R_9 (84), natural

DOI: 10.1021/am507237n
ACS Appl. Mater. Interfaces 2015, 7, 4549−4559

white CCT (4450 K), and acceptable luminous efficacy (71.1 lm/W). Moreover, the 2D PCL-assisted CPP/free-standing red film phosphor-based LED exhibited good current and thermal stability as functions of both applied current and ambient temperature, and stable angular dependence on the emission. Therefore, this combination of a 2D PCL and free-standing red film phosphor can be applied to achieve a high-power white CPP-capped LED with excellent CRI.

AUTHOR INFORMATION

Corresponding Authors

*E-mail: jzhang@jsnu.edu.cn.

*E-mail: yrdo@kookmin.ac.kr. Phone: +82-2-910-4893. Fax: +82-2-910-4415.

Notes

The authors declare no competing financial interest.

ACKNOWLEDGMENTS

This work was supported by the National Research Foundation of Korea (NRF) grant funded by the Korea government (Ministry of Science, ICT&Future Planning (MSIP)) (No. 2011-0017449), (NRF-2012M1A2A2671718), and the MSIP, Korea, under the Information Technology Research Center (ITRC) support program NIPA-2013-(H0301-13-1004) supervised by the NIPA (National IT Industry Promotion Agency).

REFERENCES

(1) Yanagida, T.; Takahashi, H.; Ito, T.; Kasama, D.; Kokubun, M.; Makishima, K.; Yanagitani, T. Evaluation of Properties of YAG (Ce) Ceramic Scintillators. *IEEE Trans. Nucl. Sci.* **2005**, *52*, 1836−1841.

(2) Podhorodecki, A.; Gluchowski, P.; Zatryb, G.; Syperek, M.; Misiewicz, J.; Lojkowski, W.; Strek, W. Influence of Pressure-Induced Transition from Nanocrystals to Nanoceramic form on Optical Properties of Ce-doped $Y_3Al_5O_{12}$. *J. Am. Ceram. Soc.* **2011**, *94*, 2135−2140.

(3) Yanagida, T.; Ito, T.; Takahashi, H.; Sato, M.; Enoto, T.; Kokubun, M.; Makishima, K.; Yanagitani, T.; Yagi, H.; Shigeta, T. Improvement of Ceramic YAG(Ce) Scintillators to $(Y,Gd)_3Al_5O_{12}$(Ce) for Gamma-Ray Detectors. *Nucl. Instrum. Methods Phys. Res., Sect. A* **2007**, *579*, 23−26.

(4) Lempicki, A.; Brecher, C.; Szupryczynski, P.; Lingertat, H.; Nagarkar, V. V.; Tipnis, S. V.; Miller, S. R. A New Lutetia-Based Ceramic Scintillator for X-ray Imaging. *Nucl. Instrum. Methods Phys. Res., Sect. A* **2002**, *488*, 579−590.

(5) Zych, E.; Hreniak, D.; Strek, W. Spectroscopic Properties of Lu_2O_3/Eu^{3+} Nanocrystalline Powders and Sintered Ceramics. *J. Phys. Chem. B* **2002**, *106*, 3805−3812.

(6) Nakamura, R.; Yamada, N.; Ishii, M. Effects of Halogen Ions on the X-ray Characteristics of Gd_2O_2S:Pr Ceramic Scintillators. *Jpn. J. Appl. Phys.* **1999**, *38*, 6923−6925.

(7) Gorokhova, E. I.; Demidenko, V. A.; Eron'ko, S. B.; Khristich, O. A.; Mikhrin, S. B.; Rodnyi, P. A. Spectrokinetic Characteristics of Gd_2O_2S:Pr, Ce Ceramics. *J. Opt. Technol.* **2006**, *73*, 130−137.

(8) Ikesue, A.; Furusato, I.; Kamata, K. Fabrication of Polycrystalline, Transparent YAG Ceramics by a Solid State Reaction Method. *J. Am. Ceram. Soc.* **1995**, *78*, 225−228.

(9) Ikesue, A.; Kamata, K.; Yoshida, K. Effects of Neodymium Concentration on Optical Characteristics of Polycrystalline Nd:YAG Laser Materials. *J. Am. Ceram. Soc.* **1996**, *79*, 1921−1926.

(10) Cherepy, N. J.; Kuntz, J. D.; Tillotson, T. M.; Speaks, D. T.; Payne, S. A.; Chai, B. H. T.; Porter-Chapman, Y.; Derenzo, S. E. Cerium-Doped Single Crystal and Transparent Ceramic Lutetium Aluminum Garnet Scintillators. *Nucl. Instrum. Methods Phys. Res., Sect. A* **2007**, *579*, 38−41.

(11) Nishiura, S.; Tanabe, S.; Fujioka, K.; Fujimoto, Y. Properties of Transparent Ce:YAG Ceramic Phosphors for White LED. *Opt. Mater.* **2011**, *33*, 688−691.

(12) Zhao, W.; Anghel, S.; Mancini, C.; Amans, D.; Boulon, G.; Epicier, T.; Shi, Y.; Feng, X. Q.; Pan, Y. B. V. chani, and A. Yoshikawa, Ce^{3+} Dopant Segregation in $Y_3Al_5O_{12}$ Optical Ceramics. *Opt. Mater.* **2011**, *33*, 684−687.

(13) Wei, N.; Lu, T.; Li, F.; Zhang, W.; Ma, B.; Lu, Z.; Qi, J. Transparent Ce: $Y_3Al_5O_{12}$ Ceramic Phosphors for White Light-Emitting Diodes. *Appl. Phys. Lett.* **2012**, *101*, 061902.

(14) Fujita, S.; Yoshihara, S.; Sakamoto, A.; Yamamoto, S.; Tanabe, S. YAG Glass-Ceramic Phosphor for White LED (I): Background and Development. *Proc. SPIE* **2005**, *5941*, 186−192.

(15) Fujita, S.; Sakamoto, A.; Tanabe, S. Luminescence Characteristics of YAG Glass-Ceramic Phosphor for White LED. *IEEE J. Sel. Top. Quantum Electron.* **2008**, *14*, 1387−1391.

(16) Narendran, N.; Gu, Y.; Freyssinier-Nova, J. P.; Zhu, Y. Extracting Phosphor-Scattered Photons to Improve White LED Efficiency. *Phys. Status Solidi A* **2005**, *202*, R60−R62.

(17) Yamada, K.; Imai, Y.; Ishii, K. Optical Simulation of Light Source Devices Composed of Blue LEDs and YAG Phosphor. *J. Light Visual Environ.* **2003**, *27*, 70−74.

(18) Park, H. K.; Oh, J. H.; Do, Y. R. Toward Scatter-Free Phosphors in White Phosphor-Converted Light-Emitting Diodes. *Opt. Express* **2012**, *20*, 10218−10228.

(19) Nishiura, S.; Tanabe, S.; Fujioka, K.; Fujimoto, Y.; Nakatsuka, M. Preparation and Optical of Transparent Ce:YAG Ceramics for High Power White LED. *IOP Conf. Ser.: Mater. Sci. Eng.* **2009**, *1*, 012031.

(20) Nishiura, S.; Tanabe, S.; Fujioka, K.; Fujimoto, Y. Preparation of Transparent Ce^{3+}:GdYAG Ceramics Phosphors for White LED. *IOP Conf. Series: Mater. Sci. Eng.* **2011**, *18*, 102005.

(21) Mao, A.; Schaper, C. D.; Karlicek, R. F., Jr Nanopatterning using a Simple Bi-Layer Lift-Off Process for the Fabrication of a Photonic Crystal Nanostructure. *Nanotechnology* **2013**, *24*, 085302.

(22) Park, H. K.; Oh, J. R.; Do, Y. R. 2D SiN_x Photonic Crystal Coated $Y_3Al_5O_{12}:Ce^{3+}$ Ceramic Plate Phosphor for High-Power White Light-Emitting Diodes. *Opt. Express* **2011**, *19*, 25593−25601.

(23) Park, B. K.; Park, H. K.; Oh, J. H.; Oh, J. R.; Do, Y. R. Selecting Morphology of $Y_3Al_5O_{12}:Ce^{3+}$ Phosphors for Minimizing Scattering Loss in the pc-LED Package. *J. Electrochem. Soc.* **2012**, *159*, J96−J106.

(24) Park, H. K.; Yoon, S. W.; Choi, D. Y.; Do, Y. R. Fabrication of Wafer-Scale TiO_2 Nanobowl Arrays via a Scooping Transfer of Polystyrene Nanospheres and Atomic Layer Deposition for Their Application in Photonic Crystals. *J. Mater. Chem. C* **2013**, *1*, 1732−1738.

(25) Yoon, S. W.; Park, H. K.; Oh, J. H.; Do, Y. R. Full Extraction of 2D Photonic Crystal Assisted $Y_3Al_5O_{12}$:Ce Ceramic Plate Phosphor for Highly Efficient White LEDs. *IEEE Photonics J.* **2014**, *6*, 8400110.

(26) Yoon, S. W.; Park, H. K.; Ko, K.-Y.; Ahn, J.; Do, Y. R. Various Nanofabrication Approaches Towards Two-Dimensional Photonic Crystals for Ceramic Plate Phosphor-Capped White Light-Emitting Diodes. *J. Mater. Chem. C* **2014**, *2*, 7513−7522.

(27) Babin, V.; Gorbenko, V.; Krasnikov, A.; Makhov, A.; Nikl, M.; Zazubovich, S.; Zorenko, Yu. Influence of Lead-Related Centers on Luminescence of Ce^{3+} and Pr^{3+} Centers in Single Crystalline Films of Aluminium Perovskites and Garnets. *Radiat. Meas.* **2010**, *45*, 415.

(28) Praveena, R.; Shi, L.; Jang, K. H.; Venkatramu, V.; Jayasankar, C. K.; Seo, H. J. Sol-Gel Synthesis and Thermal Stability of Luminescence of $Lu_3Al_5O_{12}:Ce^{3+}$ Nano-Garnet. *J. Alloys Compd.* **2011**, *509*, 859−863.

(29) Li, H.-L.; Liu, X.-J.; Huang, L.-P. Fabrication of Transparent Cerium-Doped Lutetium Aluminum Garnet (LuAG:Ce) Ceramics by a Solid-State Reaction Method. *J. Am. Ceram. Soc.* **2005**, *88*, 3226−3228.

(30) Xu, J.; Shi, Y.; Xie, J.; Lei, F. Fabrication, Microstructure, and Luminescent Properties of Ce^{3+}-Doped $Lu_3Al_5O_{12}$ (Ce:LuAG) Transparent Ceramics by Low-Temperature Vacuum Sintering. *J. Am. Ceram. Soc.* **2013**, *96*, 1930−1936.

DOI: 10.1021/am507237n
ACS Appl. Mater. Interfaces 2015, 7, 4549−4559

(31) Xu, J.; Fan, L.; Shi, Y.; Li, J.; Xie, J.; Lei, F. Effects of Ce^{3+} Doping Concentrations on Microstructure and Luminescent Properties of Ce^{3+}:$Lu_3Al_5O_{12}$ (Ce:LuAG) Transparent Ceramics. *Opt. Mater.* **2014**, *36*, 1954−1958.
(32) Xie, R.-J.; Hirosaki, N.; Kimura, N.; Sakuma, K.; Mitomo, M. 2-Phosphor-Converted White Light-Emitting Diodes using Oxynitride/Nitride Phosphors. *Appl. Phys. Lett.* **2007**, *90*, 191101.
(33) Luo, D.; Zhang, J.; Xu, C.; Yang, H.; Lin, H.; Zhu, H.; Tang, D. Yb:LuAG Laser Ceramics: a Promising High Power Laser Gain Medium. *Opt. Mater. Express* **2012**, *2*, 1425−1431.
(34) Luo, D.; Zhang, J.; Xu, C.; Lin, H.; Yang, H.; Zhu, H.; Shao, G.; Tang, D.; Kong, L. Mode-Locked Yb:LuAG Ceramics Laser. *Phys. Status Solidi C* **2013**, *10*, 967−968.
(35) Park, H. K.; Moon, J. H.; Yoon, S.; Do, Y. R. Fabrication of Micro-Patterned 2D Nanorod and Nanohole Arrays by a Combination of Photolithography and Nanosphere Lithography. *J. Electrochem. Soc.* **2011**, *158*, J143−J149.
(36) Li, H. L.; Liu, X. J.; Huang, L. P. Fabrication of Transparent Cerium-Doped Lutetium Aluminum Garnet Ceramics by Co-Precipitation Routes. *J. Am. Ceram. Soc.* **2006**, *89*, 2356−2358.
(37) Oh, J. H.; Yang, S. J.; Do, Y. R. Healthy, Natural, Efficient and Tunable Lighting: Four-Package White LEDs for Optimizing the Circadian Effect, Color Quality and Vision Performance. *Light: Sci. Appl.* **2014**, *3*, e141.
(38) Žukauskas, A.; Vaicekauskas, R.; Shur, M. S. Colour-Rendition Properties of Solid-State Lamps. *J. Phys. D: Appl. Phys.* **2010**, *43*, 354006.
(39) Davis, W.; Ohno, Y. Toward and Improved Color Rendering Metric. *Proc. SPIE* **2005**, *5941*, 59411G.
(40) Dorenbos, P. Energy of the First $4f^7 \rightarrow 4f^6 5d$ Transition of Eu^{2+} in Inorganic Compounds. *J. Lumin.* **2003**, *104*, 239−260.
(41) Smet, P. F.; Parmentier, A. B.; Poelman, D. Selecting Conversion Phosphors for White Light-Emitting Diodes. *J. Electrochem. Soc.* **2011**, *158*, R37−R54.

DOI: 10.1021/am507237n
ACS Appl. Mater. Interfaces 2015, 7, 4549−4559